



**HAL**  
open science

## Measuring the particles in fly ash by means of an image segmentation

Amelia Carolina Sparavigna

► **To cite this version:**

Amelia Carolina Sparavigna. Measuring the particles in fly ash by means of an image segmentation. *Philica*, 2017, 2017 (1105). <hal-01579285>

**HAL Id: hal-01579285**

**<https://hal.science/hal-01579285v1>**

Submitted on 30 Aug 2017

**HAL** is a multi-disciplinary open access archive for the deposit and dissemination of scientific research documents, whether they are published or not. The documents may come from teaching and research institutions in France or abroad, or from public or private research centers.

L'archive ouverte pluridisciplinaire **HAL**, est destinée au dépôt et à la diffusion de documents scientifiques de niveau recherche, publiés ou non, émanant des établissements d'enseignement et de recherche français ou étrangers, des laboratoires publics ou privés.



HAL Authorization

## Measuring the particles in fly ash by means of an image segmentation

**Amelia Carolina Sparavigna**

Department of Applied Science and Technology, Politecnico di Torino, Italy

The paper is showing how to measure, by means of the segmentation of a SEM image, the cross-sections of the particles in fly ash.

Keywords: Image processing, Segmentation of images, Size of domains, Fly ash.

As explained in [1], fly ash is a coal combustion product composed of fine particles. In the past, "fly ash was generally released into the atmosphere", but today the requirement of avoiding air pollution is imposing its capture prior to be released. In modern power plants generating fine particles from combustion, electrostatic precipitators or other filtration devices generally capture fly ash before the gases containing it reach the chimneys of the plants [1].

Thanks to Wikipedia and user Wabeggs we can see a photomicrograph made by means of a scanning electron microscope (SEM) and back-scatter detector. Here the image is reproduced in the Figure 1. Besides being very beautiful, this image is very interesting and seems useful for an elaboration, by means of an image processing, to evaluate the size of the particles we find in it. Some references which are studying the fly ash with image processing and image segmentation are given in [2-10].

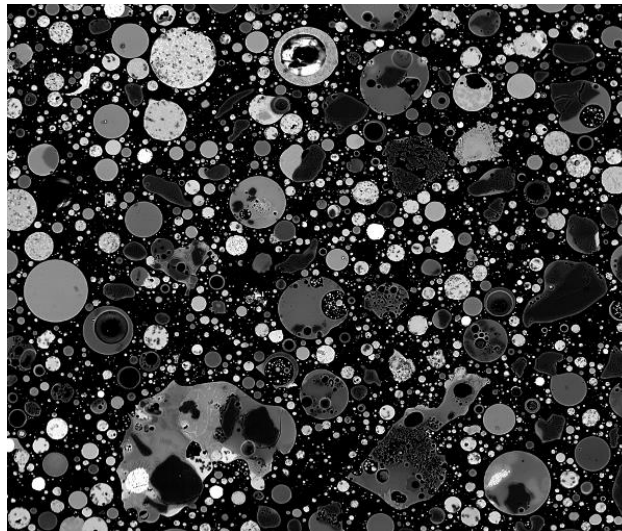


Figure 1: Thanks to Wikipedia and user Wabeggs we can see a photomicrograph made by means of a scanning electron microscope (SEM) and back-scatter detector. Here we see the image we use for processing ( 600x509 pixels ).

Here let us address a simple problem: that of measuring the cross-section of the particles that we see in the Figure 1. We measure it by means of a segmentation based on thresholding as discussed and applied in [11-16].

In image processing, a segmentation is a process of partitioning an image into multiple sets of pixels, that is, into some domains defined as “super-pixels”, in order to have a representation more useful to the following desired analyses [17-20]. The typical use of the image segmentation is that of locate objects (the domains), and find the boundaries among them. Specifically, the segmentation is a process of assigning a label to every pixel in an image, such that the pixels having the same label share certain characteristics [20]. Consequently, the result of the segmentation is a set of "segments" or “super-pixels”, covering the whole image. Here in the Figure 2 the segmentation of the Figure 1.

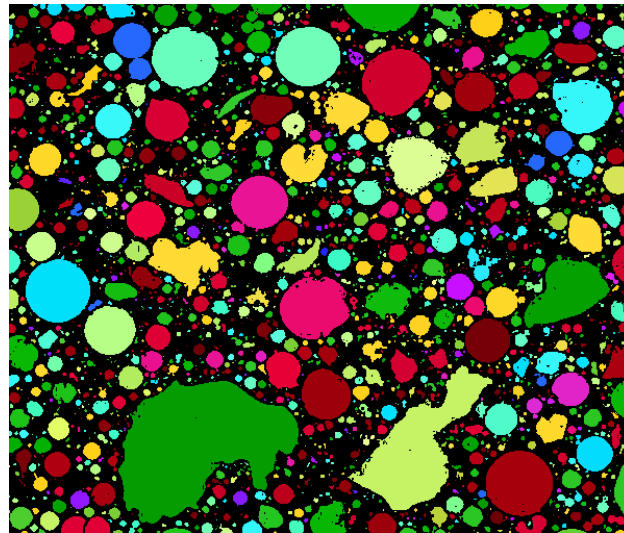


Figure 2: Result of the segmentation of the image in the Figure 1. Each domain (super-pixel) has a different colour.

The segmentation that we used to obtain the Figure 2 is based on a binary image, that is, on a black and white image obtained from that in the Figure 1. In the binary image, the domains are identified as the super-pixels, giving them different colours. The main part of the work is that of obtaining a proper binary image on which operate the segmentation.

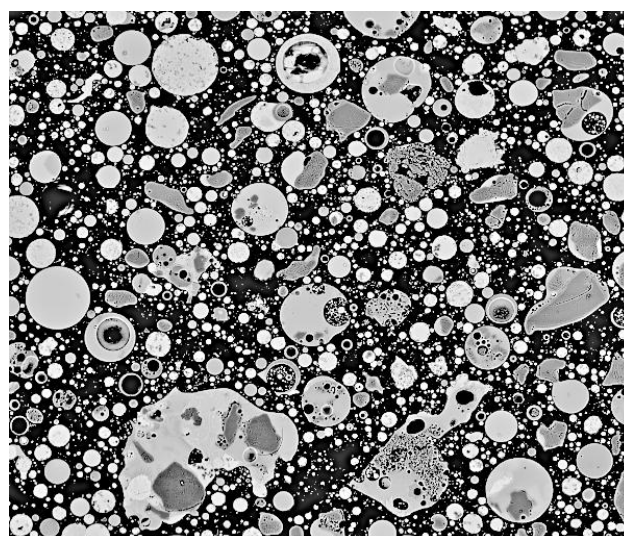


Figure 3: Effect of the pre-processing of Fig.1 by means of the GIMP Retinex filter.

For the image in the Figure 1 we need a pre-processing. It is obtained using the GIMP Retinex filter that we have used in some previous applications [21-26].

Several Retinex approaches exist [27,28]; one of them is known the MultiScale Retinex with Colour Restoration (MSRCR). GIMP Retinex is based on this approach to Retinex. It was developed by Fabien Peisson and is provided by GIMP software [29]. The resulting image of this filter can be adjusted selecting different levels, scales and dynamics. There are three “levels”: uniform, which tends to treat both low and high intensity areas fairly, low, that “flares up” the lower intensity areas on the image, and high that tends to “bury” the lower intensity areas in favour of a better rendering of the clearer areas of the image. The “scale” determines the depth of the Retinex scale. Minimum value is 16, a value providing gross, unrefined filtering. Maximum value is 250. Optimal and default value is 240. A “scale division” determines the number of iterations in the multiscale Retinex filter. The minimum required, and the recommended value is three. The “dynamic” slider allows adjusting colour saturation contamination around the new average colour (default value is 1,2). The image in the Figure 3 is obtained using the filter level LOW, Scale 240, Scale division 3 and Dynamic slider 1,2.

On the image of the Figure 3 a further processing is applied. It is obtained by the OILIFY filter of GIMP, that makes the image look like an oil painting. The Mask size allows controlling the outcome. To have the Figure 4 (on the left) we used the lowest value.

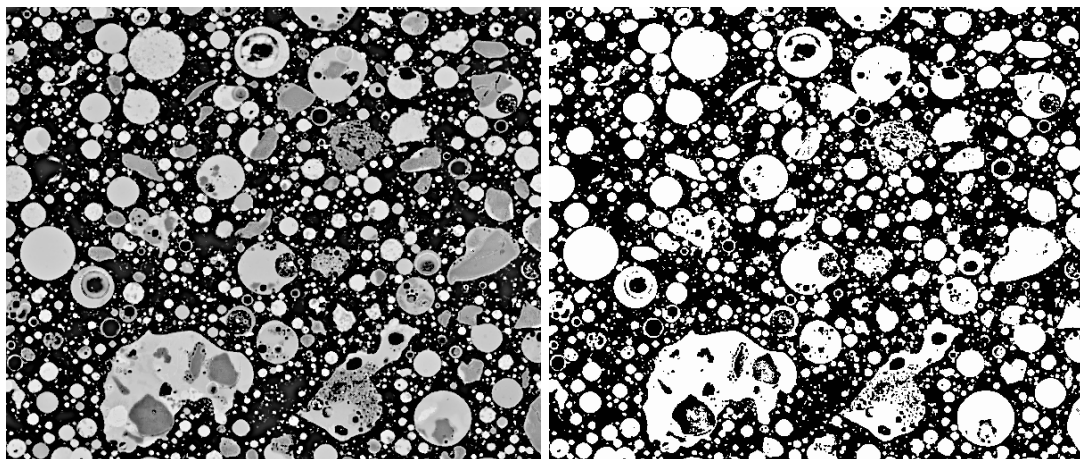


Figure 4: On the left, the image obtained using OILIFY filter of GIMP on the image in Fig.3. On the right, the binary image we obtained from this filtered image.

The image in the Figure 4 is converted into a binary image by a thresholding. We use again the GIMP software, in particular the GIMP Threshold tool. It transforms an image into a black and white image, where white pixels represent the pixels of the image the value of which is above the threshold, and black pixels represent pixels with values below the threshold. In the Figure 4, on the right, the threshold was determined to have the best choice, according to a direct visual observation.

The resulting binary image is containing white domains, the particles, in a black background. In this image, some particles are fused in the same white domain. Moreover, the particles can contain holes inside or structures inside which are not relevant for the measurement of the cross-section. Therefore, a further processing is required; in this last operation, we work by hand using Paint software. It is quite short to do. The final result is in the Figure 5. In summary, to have the binary image, we started from image I in Fig.1. We filter it using Retinex obtaining an image I'; then I' is filtered using OILIFY, having I''. I'' is converted in black and white image I''' by a Thresholding. Finally I''' is adjusted by means of Paint. Actually: I (Figure 1) → Retinex → I' → OILIFY → I'' → T → I''' → Paint → I'''' (Figure 5).

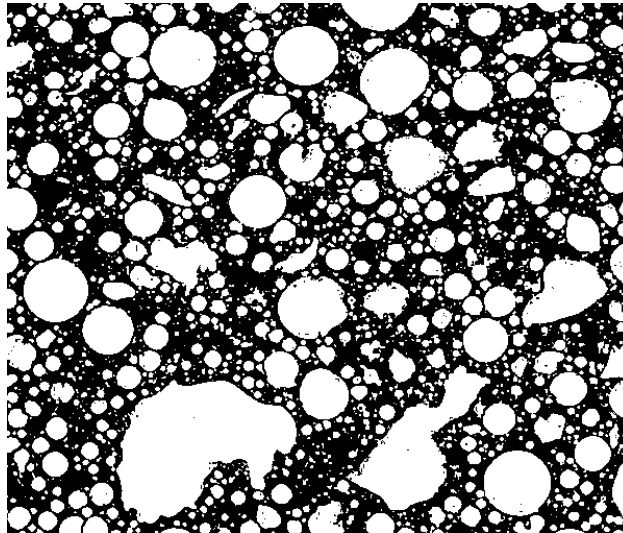


Figure 5: Here the binary image the segmentation of which is given in the Figure 2.

After having determined the coloured domains, it is easy to obtain the cross-section of each of them. The cross-section is the number of pixels contained in the domain. If we have the possibility to know the measure, in microns, of the image size, it is very simple to estimate the area (in microns) of the domains. Moreover, we can determine the distribution of the domains, that is, the distribution of the cross-sections of the particles in the SEM image, by counting them according to their area within intervals spaced of a certain amount of pixels. Here the original image is scaled to 600x509 pixels, in order to reduce the time of computation, and the areas are spaced of 10 pixels. We obtain the distribution given in the Figure 6.

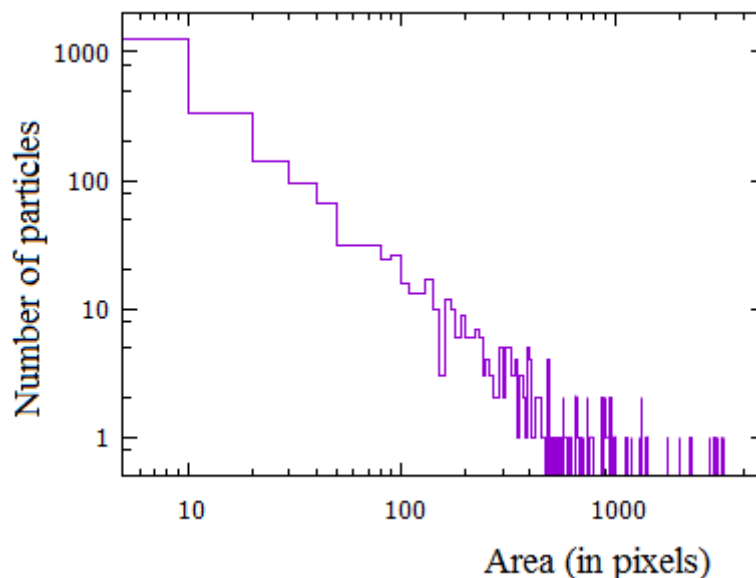


Figure 6: Distribution of the cross-sections of particles. In this diagram, we have not considered the two largest irregular particles (green and pale green) of the Figure 2. The area are spaced in intervals of 10 pixels.

As we can see, there is a large amount of very small particles. From the area of particles, since they are almost spherical a distribution of diameters can be deduced too. Moreover, on the data obtained from the segmentation, we have the possibility of making further statistical studies, which are under consideration.

Let us conclude showing another example of segmentation on an image from Wikipedia, user Shinkolobwe (Figure 7). It is another photomicrograph made with a Scanning Electron Microscope.

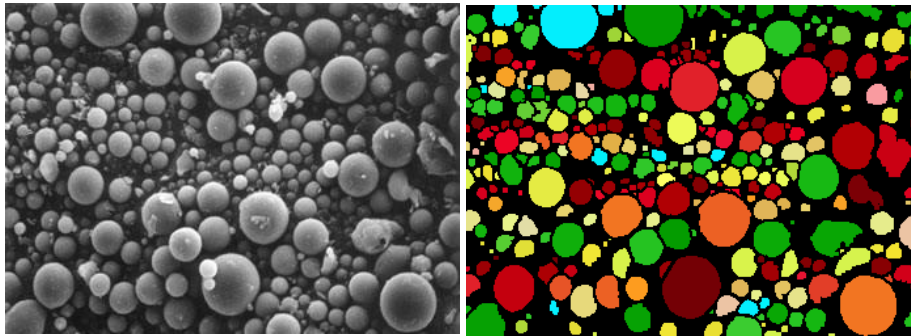


Figure 7: Thanks to Wikipedia and user Shinkolobwe we can see another example of segmentation of a SEM photomicrograph of fly ash.

## References

- [1] Vv. Aa. (2017). Fly-ash. Wikipedia. [https://en.wikipedia.org/wiki/Fly\\_ash](https://en.wikipedia.org/wiki/Fly_ash)
- [2] Coudray, N., Dieterlen, A., Roth, E., & Trouvé, G. (2009). Density measurement of fine aerosol fractions from wood combustion sources using ELPI distributions and image processing techniques. *Fuel*, 88(5), 947-954.
- [3] Deschner, F., Münch, B., Winnefeld, F., & Lothenbach, B. (2013). Quantification of fly ash in hydrated, blended Portland cement pastes by backscattered electron imaging. *Journal of microscopy*, 251(2), 188-204.
- [4] Coudray, N., Dieterlen, A., Vidal, L., Roth, E., Trouvé, G., & Bistac, S. (2008). Image processing nanoparticle size measurement for determination of density values to correct the ELPI measures. *Precision engineering*, 32(2), 88-99.
- [5] Soroushian, P., & Elzafraney, M. (2005). Morphological operations, planar mathematical formulations, and stereological interpretations for automated image analysis of concrete microstructure. *Cement and Concrete Composites*, 27(7), 823-833.
- [6] Lanzón, M., Cnudde, V., De Kock, T., & Dewanckele, J. (2012). X-ray microtomography ( $\mu$ -CT) to evaluate microstructure of mortars containing low density additions. *Cement and Concrete Composites*, 34(9), 993-1000.
- [7] Barrioulet, M., Cros, H., Husson, B., & Ringot, E. (1994). Image Analysis of Fly Ash in the Characterization of the Shape of the Grains. *MRS Online Proceedings Library Archive*, 370.
- [8] Szponder, D. K., & Trybalski, K. (2011). Application of computer image analysis and scanning electron microscopy in environmental engineering and waste management. *Challenges of Modern Technology*, 2(2), 56-62.
- [9] Moon, J., Bae, S., Celik, K., Yoon, S., Kim, K. H., Kim, K. S., & Monteiro, P. J. (2014). Characterization of natural pozzolan-based geopolymeric binders. *Cement and Concrete Composites*, 53, 97-104.
- [10] Deschner, F. (2014). Reaction of siliceous fly ash in blended Portland cement pastes and its effect on the chemistry of hydrate phases and pore solution (Doctoral dissertation, Friedrich-Alexander-Universität Erlangen-Nürnberg (FAU)).
- [11] Sparavigna, A. C. (2017). Image Segmentation Applied to the Study of Micrographs of Cellular Solids, *International Journal of Sciences*, 6(2), 68-76. DOI: 10.18483/ijSci.1201
- [12] Sparavigna, A. C. (2017). Image segmentation applied to micrographs of microcellular plastics. *Philica*, 2017, n.953. <hal-01456692>

- [13] Sparavigna, A. C. (2016). Analysis of a natural honeycomb by means of an image segmentation. *Philica*, 2016, n.897. <hal-01416832>
- [14] Sparavigna, A. C. (2016). A method for the segmentation of images based on thresholding and applied to vesicular textures. *arXiv preprint arXiv:1612.01131*.
- [15] Sparavigna, A. C. (2017). Measuring the size of tubules in phloem and xylem of plants. *Philica*, 2017, n.1104. <hal-01578826>
- [16] Sparavigna, A. C., Pisano, R., & Barresi, A. A. (2017). Measuring the size of pores by the segmentation of images from scanning electron microscopy. *6th European Drying Conference (EuroDrying 2017)*, Jun 2017, Liège, Belgium.
- [17] Shapiro, L. G., & Stockman, G. C. (2001). *Computer vision*, New Jersey, Prentice-Hall, ISBN 0-13-030796-3
- [18] Pham, D. L., Xu, Chenyang, & Prince, J. L. (2000). Current methods in medical image segmentation. *Annual Review of Biomedical Engineering* 2, 315–337.
- [19] Forghani, M., Forouzanfar, M., & Teshnehlal, M. (2010). Parameter optimization of improved fuzzy c-means clustering algorithm for brain MR image segmentation. *Engineering Applications of Artificial Intelligence*, 23 (2): 160–168.
- [20] Vv. Aa. (2016). Wikipedia. [https://en.wikipedia.org/wiki/Image\\_segmentation](https://en.wikipedia.org/wiki/Image_segmentation)
- [21] Sparavigna, A. C. (2015). Retinex filtering and thresholding of foggy images. *PHILICA.COM* Article number 511.
- [22] Sparavigna, A. C., & Marazzato, R. (2015). Effects of GIMP Retinex Filtering Evaluated by the Image Entropy. *arXiv preprint arXiv:1512.05653*.
- [23] Marazzato, R., & Sparavigna, A. C. (2015). Retinex filtering of foggy images: generation of a bulk set with selection and ranking. *arXiv preprint arXiv:1509.08715*.
- [24] Sparavigna, A. C. (2015). GIMP Retinex for enhancing images from microscopes. *International Journal of Sciences*, 4(6), 72-79. DOI: 10.18483/ijsci.758
- [25] Sparavigna, A. C. (2015). An image processing approach based on Gnu Image Manipulation Program GIMP to the panoramic radiography. *International Journal of Sciences*, 4(5), 57-67. DOI: 10.18483/ijsci.721
- [26] Sparavigna, A. C., & Marazzato, R. (2017). The GIMP Retinex Filter Applied to the Fabric Fault Detection. *International Journal of Sciences*, 6(03), 106-112. DOI: 10.18483/ijSci.1227
- [27] Jobson, D.J., Rahman, Z., & Woodell, G.A. (1997). A Multi-Scale Retinex for bridging the gap between colour images and the human observation of scenes, *IEEE Transactions on Image Processing*, 6(7), 965-976.
- [28] Jobson, J., Rahman, Z., & Woodell, G.A. (1997). Properties and performance of a center/surround Retinex, *Image Processing IEEE Transactions on*, 6(3), 451-462.
- [29] Fabien Pelisson, GIMP Retinex, <http://www-prima.inrialpes.fr/pelisson/MSRCR.php>